Angular distribution of electrons elastically scattered from Ar in the presence of a 1.17 eV laser field

N. L. S. Martin, C. M. Weaver, B. N. Kim, and B. A. deHarak

The angular distribution of electrons elastically scattered from Ar in the presence of a 1.17 eV laser field

N. L. S. Martin,[1] C. M. Weaver,[1] B. N. Kim,[1] and B. A. deHarak[2]

[1]Department of Physics and Astronomy,

University of Kentucky, Lexington, Kentucky 40506-0055, USA

[2]Physics Department, Illinois Wesleyan University,

P.O. Box 2900, Bloomington, IL 61702-2900, USA

Abstract

Experiments on free-free electron scattering by an Ar target are reported. The angular distribution of 350 eV electrons, elastically scattered at angles between 4° and 80° in the presence of 1.17 eV photons from a Nd:YAG laser, shows a pronounced maximum close to 47°, and is symmetric about this angle, as predicted by a Kroll-Watson approximation calculation for the experimental kinematics. The experiments test a term in the approximation that is a strong function of the magnitude and direction of the momentum transfer of the elastically scattered electrons.

PACS numbers: 34.80.Dp

I. INTRODUCTION

The free-free process is the scattering of an unbound charged particle by an atom, molecule, or ion, accompanied by the absorption (or emission) of energy, from (or into) an ambient electromagnetic field [1, 2]. It is of interest, not only as a fundamental phenomenon, but also because of its importance in astrophysical and plasma modeling. This has been known since the 1930's: Pannekoek [3] found that free-free transitions affect the infrared opacities of certain types of stars [4], and Chandrasekhar and Breen [5] found that free-free processes, for electrons on negative hydrogen ions, were important in the long wavelength absorption by the solar atmosphere. Free-free transitions dominate the radiation transport in air plasmas, such as cascade arcs and shock tubes [6], and such transitions are also important in plasma heating by radiation [7]. More recently, Kirchner [8] proposed the use of laser-assisted collision processes to manipulate ionization and capture in ion-atom collisions.

The free-free process may be conveniently studied in the laboratory using a crossed-beam type apparatus with an interaction region formed by the intersection of a charged-particle beam, a gas-jet target, and a laser beam. The first such experiments on electron scattering in a laser field were carried out using a continuous CO_2 laser by Andrick and Langhans [9] who observed single 0.117 eV photon emission and absorption by an electron scattered elastically from Ar. Similar experiments by Weingartshofer *et al.* [10] observed the absorption and emission of up to three 0.117 eV photons during e–Ar elastic scattering in the presence of a pulsed CO_2 laser. Wallbank and Holmes [11–13] later carried out similar experiments using a pulsed CO_2 laser and helium and argon targets; they reported the absorption and emission of up to five 0.117 eV photons. Mason and Newell [14] carried out the first experiment on electron impact *excitation* in the presence of a CO_2 laser field (simultaneous electron-photon excitation, or SEPE), and Luan *et al.* [15] investigated SEPE in He using a Nd:YAG laser which produces photons of energy 1.17 eV, ten times the CO_2 laser energy. In a very challenging $(e,2e)$ experiment, Höhr *et al.* [16] investigated He ionization by 1 keV electrons in the presence of a laser field of 1.17 eV photons from a Nd:YAG laser.

In our experiments the charged particles are electrons, and an Nd:YAG laser produces 1.17 eV photons. The reaction studied is

$$A + e(E_0) + \mathcal{N}\hbar\omega \rightarrow A' + e(E) + \mathcal{N}'\hbar\omega, \tag{1}$$

where an electron of energy E_0 is incident on a target A in the presence of a laser field of frequency ω, and $\mathcal{N}' = \mathcal{N} \pm \ell$, corresponds to the emission $(+)$ or absorption $(-)$ of ℓ photons by the $A + e$ system, resulting in a final electron energy $E = E_0 \mp \ell \hbar \omega$.

Laser-assisted free-free processes have been fairly successfully described by the semiclassical Kroll-Watson Approximation (KWA) [17]. Our previous experiments tested the dependance of the KWA on (i) the incident electron energy [18], (ii) the direction of the laser polarization [19], and (iii) the target species [20]; we recently reviewed these investigations into the validity of the KWA [21]. In this paper, we present our latest experiment into the validity of the KWA; it examines the angular dependance of the free-free signal for electrons elastically scattered through a range of angles by an Ar target in the presence of a 1.17 eV laser beam.

Section II gives the Kroll-Watson approximation and our previous experimental tests of it, discusses deviations due to dressing effects of the target by the laser field, and discusses their possible effect on the present experiments. Section III describes the apparatus and the geometry of our free-free measurements. Section IV presents the results, and Section V contains our summary and conclusions.

II.   THEORY

A.   Kroll-Watson Approximation

The KWA relates the free-free cross section $d\sigma_{FF}^{(\ell)}/d\Omega$, for absorption $(\ell < 0)$ or emission $(\ell > 0)$ of ℓ photons, to the field-free elastic-scattering cross section $d\sigma_{el}/d\Omega$, by [17]

$$\frac{d\sigma_{FF}^{(\ell)}}{d\Omega} = \frac{k_f}{k_i} J_\ell^2(x) \frac{d\sigma_{el}}{d\Omega}. \tag{2}$$

Here $\boldsymbol{k}_i$ and $\boldsymbol{k}_f$ are the initial and final electron momenta, and J_ℓ is a Bessel function of the first kind of order ℓ, with argument

$$x = -0.022 \lambda^2 I^{1/2} E_i^{1/2} \frac{\hat{\boldsymbol{\epsilon}} \cdot \boldsymbol{Q}}{k_i}, \tag{3}$$

where λ is the wavelength of the radiation in μm, I is its intensity in GW/cm^2, $\hat{\boldsymbol{\epsilon}}$ is the polarization direction, E_i is the incident electron energy in eV, and $\boldsymbol{Q} = \boldsymbol{k_i} - \boldsymbol{k_f}$ is the momentum transfer. In fact what is measured in an experiment is the ratio of the free-free

(laser-on) cross section to the elastic scattering (laser-off) cross section,

$$(d\sigma_{FF}^{(\ell)}/d\Omega)/(d\sigma_{el}/d\Omega) = \frac{k_f}{k_i} J_\ell^2(x), \tag{4}$$

which provides a direct test of the KWA, independent of a knowledge of the scattering cross section. In the limit of small x, the Bessel function may be approximated by the first term of a power series expansion and Eq. (4) becomes

$$(d\sigma_{FF}^{(\ell)}/d\Omega)/(d\sigma_{el}/d\Omega) \approx \frac{k_f}{k_i} \left(\frac{1}{|\ell|!}\right)^2 \left(\frac{x}{2}\right)^{2|\ell|}. \tag{5}$$

In fact this form is useful for obtaining a qualitative description of the expected free-free signal even when x is not very small.

We have carried out two experiments that probe the details of Eq. 4 for single photon processes, $i.e.$, for $\ell = \pm 1$. For a given laser wavelength and intensity, since $E_i^{1/2} \propto k_i$, the free-free signal is determined by the behavior of $\hat{\boldsymbol{\epsilon}} \cdot \boldsymbol{Q}$ in Eq. 3. Our first experiment [18], carried out at fixed laser polarization and electron scattering angle, tested the energy dependence of the KWA. For that experiment $E_i = 50 \to 350$ eV, and thus $E_i \gg \hbar\omega$. Consequently $k_f \approx k_i$, so $Q \propto k_i$ (with $\hat{\boldsymbol{Q}}$ constant), and the energy dependence enters through $x \propto E_i^{1/2}$. Our second test [19] kept the scattering kinematics fixed for each experiment and varied the laser polarization over $\theta = 0 \to 2\pi$, where θ is the angle between the polarization and the momentum-transfer direction, so that $\hat{\boldsymbol{\epsilon}} \cdot \hat{\boldsymbol{Q}} = \cos\theta$ determined the variation in the free-free signal. It was found that the KWA gave a good description of the results of both tests.

B. Dressing Effects

One of the most remarkable things about the KWA is that it predicts that the properties of the target do not affect the free-free signal. We have tested one aspect of this and have found it to be true for experiments carried out in He, Ar, and N_2 [20] at a single scattering angle of 90°.

In the derivation of the KWA, the wavefunctions of the incident and scattered electrons of charge e, mass m, wavevectors $\boldsymbol{k}_{i,f}$, are taken as the solutions of Schrödinger's equation in the laser field F,

$$\psi_{i,f}^{(F)} = \psi_{i,f}^{(0)} \times \exp\left(-i\frac{e}{m\omega^2}\mathbf{F} \cdot \mathbf{k}_{i,f}\right), \tag{6}$$

where $\boldsymbol{F}(t) = \boldsymbol{F}_0 \sin(\omega t)$ is the electric field of the laser, and $\psi_{i,f}^{(0)}$ are the field-free wavefunctions for $\boldsymbol{k}_{i,f}$. The spatial integration in the scattering matrix element involves only the $\psi_{i,f}^{(0)}$ and leads directly to the field-free $d\sigma_{el}/d\Omega$ term in Eq. 2, and an expansion of the exponential term leads to the Bessel function term [22] with $\boldsymbol{Q} = \boldsymbol{k_f} - \boldsymbol{k_i}$. (Note that two terms in the square of the field, that do not depend on $\boldsymbol{k}$, have been omitted from Eq. 6; these are eliminated by the inner product when factored out of the matrix element [22].)

This derivation of the KWA assumes that only the free electron is affected by the laser field via Eq. 6, and that the laser does not interact with the target in any way – *i.e.,* the target is not "dressed" by the laser field, and the field-free atomic wavefunction may be used.

To include dressing effects requires the use of an atomic wavefunction which is a solution of Schrödinger's equation in the laser field. Qualitatively, this corresponds to Stark mixing of the atomic energy levels, and a calculation of the absorption or emission of photons during elastic scattering requires a wavefunction that is an admixture of the ground state and opposite parity excited states. The admixture of each excited state ϕ_ν with the ground state ϕ_0 is determined by $\langle\phi_\nu|e\boldsymbol{F}_0 \cdot \boldsymbol{r}|\phi_0\rangle/(E_\nu - E_0)$, *i.e.,* by the off-diagonal dipole matrix element connecting the two states in the Hamiltonian, divided by their energy separation.

It is convenient to discuss dressing effects in terms of a Born approximation calculation in which case the free-free amplitude is the KWA amplitude modified by the addition of an extra term that is the derivative of the Bessel function, $J_\ell'(x)$, times a sum over ν of the products of the dipole-allowed Born excitation amplitudes and the excited state coefficients,

$$\frac{8\pi}{Q^2} \frac{\langle\phi_\nu| \exp(i\boldsymbol{Q} \cdot \boldsymbol{r})|\phi_0\rangle\langle\phi_\nu|e\boldsymbol{F}_0 \cdot \boldsymbol{r}|\phi_0\rangle}{E_\nu - E_0}, \tag{7}$$

and equivalent expressions with $\phi_\nu \longleftrightarrow \phi_0$ [23].

For small elastic scattering angles the Born amplitude can be expanded in powers of Q, and for $Q \ll 1$ (in atomic units) the Born matrix elements become $\langle\phi_\nu|\boldsymbol{Q} \cdot \boldsymbol{r}|\phi_0\rangle$, which are of the same form as the dipole matrix elements. For the special case of $\boldsymbol{Q}$ parallel to $\boldsymbol{F}_0$, with laser polarization defined to be in the z direction, the additional term in the free-free scattering amplitude becomes proportional to the electric dipole polarizability of the ground state,

$$\alpha = \sum_\nu \frac{|\langle\phi_\nu|ez|\phi_0\rangle|^2}{E_\nu - E_0}. \tag{8}$$

5

This leads to a cross section given by Zon [24, 25] as the polarizability α,

$$\frac{d\sigma_{ZON}^{(\ell)}}{d\Omega} = \frac{k_f}{k_i} \left| J_\ell(x)f_{el} - \frac{\alpha m_e^2 \omega^2 x}{2\pi\varepsilon_0 Q^2} J'_\ell(x) \right|^2 , \qquad (9)$$

where f_{el} is the field-free scattering amplitude $(d\sigma_{el}/d\Omega = |f_{el}|^2)$.

Byron and Joachain [23] carried out calculations of dressing effects for H ($\alpha = 4.5$ a.u.) and He ($\alpha = 1.4$ a.u.) using terms of the form of Eq. 7, and predicted sizeable cross sections, for an incident electron beam of 100 eV and scattering angles below 4°, whereas the KWA predicted essentially zero free-free cross sections.

Morimoto *et al.* [25] carried out the first experiments that unambiguously observed dressing effects in free-free collisions. For a Xe target, for which $\alpha = 28$ a.u. [26], and with 1 keV electrons, the effect of dressed states was observed at scattering angles less than 1°, and were in good agreement with a Zon-type calculation. In an earlier experiment [27] they verified that the KWA appeared to be valid between 2°, and their experimental maximum scattering angle of 12°.

C. Free-free angular distributions in Ar

Here we report new experiments that examine the free-free signal as a function of the scattering angle for single photon processes in Ar. This probes the dependance of Eq. 4 on both the magnitude and the direction of $\boldsymbol{Q}$ for a fixed incident electron energy. Note that all our previous experiments were carried out at fixed scattering angles, so the present experiment is our first to test this aspect of the KWA.

It is unclear whether we expect to see any dressing effects. Ar has a relatively small dipole polarizability, $\alpha = 11$ a.u. [26], and for experimental reasons we are restricted to scattering angles much greater than 1°. For such large scattering angles a Zon-type calculation in terms of α is not valid, and a full calculation using the terms of Eq. 7 would be necessary, requiring a detailed knowledge of excitation matrix elements. However, the lowest excited state has an excitation energy half that of He, and there are twice as many dipole-allowed excited states: $3p \rightarrow ns, nd$ as opposed to only $1s \rightarrow np$ for He. Thus we expect any dressing effects in the free-free *amplitude* for Ar at large scattering angles to be about a factor of four larger than those in He; an experimental measurement of the free-free angular distribution in Ar to test for deviations from the KWA is therefore desirable.

Figure 1 shows angular distributions for $\ell = \pm 1$ calculated with the KWA using Eq. 4, for the kinematics appropriate to our experimental setup described in the next section in which the laser polarization direction lies in the scattering plane at a nominal angle of 135° to the electron beam. Three calculations are shown, for laser intensities $I = 10$, 50, and 100 GW/cm^2, with all calculations normalized to unity at the maximum value that occurs at 45°. For intensities below 10 GW/cm^2 the (normalized) angular distributions are essentially identical, and we have therefore labeled the 10 GW/cm^2 calculation as <10 GW/cm^2; our experiments are carried out under these conditions. As can be seen in the figure, the effect of increasing the laser intensity is to broaden the angular distribution. For very high intensities above 200 GW/cm^2 (not shown), a shallow minimum appears at 45°.

The qualitative behavior of the calculated angular distributions shown in fig. 1 can be explained as follows. For zero degree scattering with $E_i = 350$ eV and an energy loss (or gain) of 1.17 eV corresponding to a single photon process, $Q \approx 0$, and the free-free cross-section vanishes. At 90° scattering the momentum transfer direction $\hat{\boldsymbol{Q}}$ is perpendicular to the laser polarization direction $\hat{\boldsymbol{\epsilon}}$, and the free-free cross-section again vanishes. In fact it is straightforward to show that for this special laser polarization direction, the quantity $\hat{\boldsymbol{\epsilon}} \cdot \boldsymbol{Q}$, and hence the free-free signal, between 0° and 90° is symmetric about 45°.

III. EXPERIMENTAL METHOD

The free-free experiments were carried out using a Continuum Powerlite 9030 Nd:YAG laser with photon energy 1.17 eV (λ=1.06 μm), repetition rate 30 Hz, pulse duration ≈ 12 ns, and, in the present experiments, intensities of order 10 GW/cm^2. (The pulse width and the intensity depend on the age of the laser flashlamps; so care had to be taken that data was taken over a time interval for which the laser intensity was constant.) The 1 cm diameter laser beam enters the vacuum chamber through a window, passes through a lens that focuses it down to 0.75 mm at the interaction region, and then expands to about 1 cm before being directed vertically upward to an exit window in the lid of the vacuum chamber. The laser beam is terminated in a beam dump with an attached thermocouple to monitor the beam intensity as a function of time. The temperature of the beam dump with the laser on is typically between 30° and 50° C above room temperature, again depending on the state of the laser flashlamps.

The kinematics of the present experiments are different from our previous experiments. In order to carry out measurements for a range of scattering angles less than 90°, the apparatus was reconfigured to the arrangement shown in fig. 2. The incident electron energy for the present experiments was fixed at $E_i = 350$ eV. The electron spectrometer consists of an unmonochromated electron gun, with an energy full-width-at-half-maximum (FWHM) of about 0.5 eV, and a scattered electron detector, both mounted on independent coplanar concentric turntables, and a single-bore gas nozzle to create the target beam; the pressure in the gas jet is estimated to be somewhat less than 1 Torr. See [18] for details of the spectrometer, data acquisition system, and data analysis.

The scattering geometry for the present experiments is as shown in fig. 2. The magnitude of the angle between the electron beam and the laser beam is nominally 135°, as it is for the polarization direction $\hat{\varepsilon}$, and the scattered electron detector is positioned to receive electrons elastically scattered through 0° to 90°– the maximum range permitted with this arrangement. The angular range of the momentum-transfer direction $\hat{\boldsymbol{Q}}$ is then as shown in the figure; the angle between $\hat{\varepsilon}$ and $\hat{\boldsymbol{Q}}$ ranges from approximately 45° to 90°.

In fact it is difficult to position the laser at exactly 135° with respect to the electron beam because the laser beam diameter varies across the vacuum chamber. After aligning the laser so that it passes exactly through the interaction region formed by the intersection of the electron beam and the gas jet, the overall path of the laser beam was measured and found to be at 137° ± 2° with respect to the electron beam. Thus the laser polarization direction is 133° ± 2° with respect to the electron beam. This systematic uncertainty includes a contribution from the alignment of the electron gun.

IV.   RESULTS AND DISCUSSION

Experiments were carried out for scattering angles between 4° and 80°. The scattered-electron detector was manually positioned at the required angle for each experiment and the electron gun was tuned to yield a count rate that could be handled by the detector electronics, in practice a maximum of 60,000 c/s in the wings of the elastic peak at an energy 1.17 eV away from the center of the elastic peak. The measured count rate in the elastic peak was then of order 10^6 c/s. The differential cross section of Ar varies by almost three orders of magnitude between 0° and 90° [28, 29], and the electron-beam current was

adjusted appropriately using the bias on the cathode housing. Each free-free experiment took of order 1 to 3 days to obtain adequate statistics. The resulting free-free angular distribution is shown in fig. 3. Two sets of data points are shown. The circles (red) are for experiments carried out using an argon atomic beam with a pressure about 1 Torr, and the squares (blue) are three experiments at about 0.1 Torr. These two pressures differing by a factor of 10 were used to check for double-scattering effects; it is known that free-free experiments can be influenced by such effects at high pressures [30]. The fact that the two pressures give the same results to within the statistical errors indicates that such effects are not present, or, if they are, do not alter the shape of the angular distribution. Note that the vertical scale is absolute, and is the number of laser-on single photon free-free counts per hour, divided by the number of electrons per hour scattered elastically when the laser is off. Thus the high and low pressure data may be directly compared.

On the other hand, the KWA may not be compared directly with the data because the exact overlap of the laser beam, electron beam, and gas jet (the geometric efficiency) is not known. We therefore fit the overall magnitude of the calculated KWA to the experiment. The solid (green) curve in fig. 3 is a fitted KWA calculation with an angle between the polarization of the laser and the electron beam of 133°, for which the fit has a satisfactory reduced chi-square $\chi^2 = 1.5$. (Note that there is an uncertainty of $\pm 2°$ in the alignment, and a better fit with $\chi^2 = 1$ can be obtained for an angle 132°.) The calculation used an intensity of 5.6 GW/cm^2, in keeping with our earlier experiments [18]. Thus the calculations fall into the < 10 GW/cm^2 range of fig. 1.

V. SUMMARY AND CONCLUSIONS

We have carried out angular distribution measurements over a wide angular range for the elastic scattering of electrons from Ar in the presence of a 1.17 eV laser field, and have compared the results with KWA calculations. The measurements correspond to an angle between the electron beam and laser polarization of 133° for which an angular distribution symmetric about 47° scattering angle is predicted; our results are close to being symmetric about this angle. Thus, within the systematic and statistical uncertainties, the measurements are rather well reproduced by the KWA model concerning the shape of the angular distributions. That might indicate that the aforementioned dressing effects are negligible in

9

the present experiment.

Future work includes carrying out free-free measurements for *inelastic* scattering in Ar. The lowest excited states have electric dipole polarizabilities of $\alpha \approx 300$ [31], and a Zon-type model predicts large cross sections via dressing effects at small angles for which the KWA predicts very small cross sections. Also, now that the present experiments have confirmed the validity of the KWA for large angle scattering in Ar, there is the possibility of observing deviations due to dressing effects for large angle inelastic scattering.

Acknowledgments

[1] N. J. Mason, Rep. Prog. Phys. **56**, 1275 (1993).

[2] F. Ehlotzky, A. Jaroń, and J. Kamiński, Phys. Rep. **297**, 63 (1998).

[3] A. Pannekoek, Monthly Notices of the Royal Astronomical Society **91**, 139 (1930).

[4] J. L. Stilley and J. Callaway, Astrophys. J. **160**, 245 (1970).

[5] S. Chandrasekhar and F. H. Breen, Astrophys. J. **104**, 430 (1946).

[6] D. Schlüter, Z. Phys. D **6**, 249 (1987).

[7] Y. Shima and H. Yatom, Phys. Rev. A **12**, 2106 (1975).

[8] T. Kirchner, Phys. Rev. Lett. **89**, 093203 (2002).

[9] D. Andrick and L. Langhans, J. Phys. B **9**, L459 (1976), URL http://stacks.iop.org/0022-3700/9/i=15/a=006.

[10] A. Weingartshofer, J. K. Holmes, G. Caudle, E. M. Clarke, and H. Krüger, Phys. Rev. Lett. **39**, 269 (1977).

[11] B. Wallbank and J. K. Holmes, Phys. Rev. A **48**, R2515 (1993).

[12] B. Wallbank and J. K. Holmes, J. Phys. B **27**, 1221 (1994).

[13] B. Wallbank and J. K. Holmes, J. Phys. B **27**, 5405 (1994).

[14] N. J. Mason and W. R. Newell, J. Phys. B **20**, L323 (1987).

[15] S. Luan, R. Hippler, and H. O. Lutz, J. Phys. B **24**, 3241 (1991).

[16] C. Hohr, A. Dorn, B. Najjari, D. Fischer, C. D. Schroter, and J. Ullrich, Phys. Rev. Lett. **94**, 153201 (pages 4) (2005), URL `http://link.aps.org/abstract/PRL/v94/e153201`.

[17] N. M. Kroll and K. M. Watson, Phys. Rev. A **8**, 804 (1973).

[18] B. A. deHarak, L. Ladino, K. B. MacAdam, and N. L. S. Martin, Phys. Rev. A **83**, 022706 (2011).

[19] B. A. deHarak, B. Nosarzewski, M. Siavashpouri, and N. L. S. Martin, Phys. Rev. A **90**, 032709 (2014).

[20] N. L. S. Martin and B. A. deHarak, Phys. Rev. A **93**, 013403 (2016), URL `https://link.aps.org/doi/10.1103/PhysRevA.93.013403`.

[21] N. L. S. Martin, C. M. Weaver, B. N. Kim, and B. A. deHarak, Journal of Physics B: Atomic, Molecular and Optical Physics **51**, 134003 (2018), URL `http://stacks.iop.org/0953-4075/51/i=13/a=134003`.

[22] N. K. Rahman, Phys. Rev. A **10**, 440 (1974), URL `https://link.aps.org/doi/10.1103/PhysRevA.10.440`.

[23] F. W. Byron Jr and C. J. Joachain, J. Phys. B **17**, L295 (1984).

[24] B. A. Zon, JETP **46(1)**, 65 (1977).

[25] Y. Morimoto, R. Kanya, and K. Yamanouchi, Phys. Rev. Lett. **115**, 123201 (2015), URL `http://link.aps.org/doi/10.1103/PhysRevLett.115.123201`.

[26] P. Schwerdtfeger, *Atomic Static Dipole Polarizabilities, in Computational Aspects of Electric Polarizability Calculations: Atoms, Molecules and Clusters, ed. G. Maroulis* (IOS Press, Amsterdam, 2006), updated 2015 at: http://ctcp.massey.ac.nz/dipole-polarizabilities.

[27] R. Kanya, Y. Morimoto, and K. Yamanouchi, Phys. Rev. Lett. **105**, 123202 (2010), URL `https://link.aps.org/doi/10.1103/PhysRevLett.105.123202`.

[28] R. D. DuBois and M. E. Rudd, Journal of Physics B: Atomic and Molecular Physics **9**, 2657 (1976), URL `http://stacks.iop.org/0022-3700/9/i=15/a=016`.

[29] A. Jablonski, F. Salvat, and C. J. Powell, National Institute of Standards and Technology, Gaithersburg, MD (2010), URL `http://www.nist.gov/srd/nist64.cfm`.

[30] B. A. deHarak, B. N. Kim, C. M. Weaver, N. L. S. Martin, M. Siavashpouri, and B. Nosarzewski, Plasma Sources Science and Technology **25**, 035021 (2016), URL `http://stacks.iop.org/0963-0252/25/i=3/a=035021`.

[31] E. Pollack, E. J. Robinson, and B. Bederson, Phys. Rev. **134**, A1210 (1964), URL `https:`
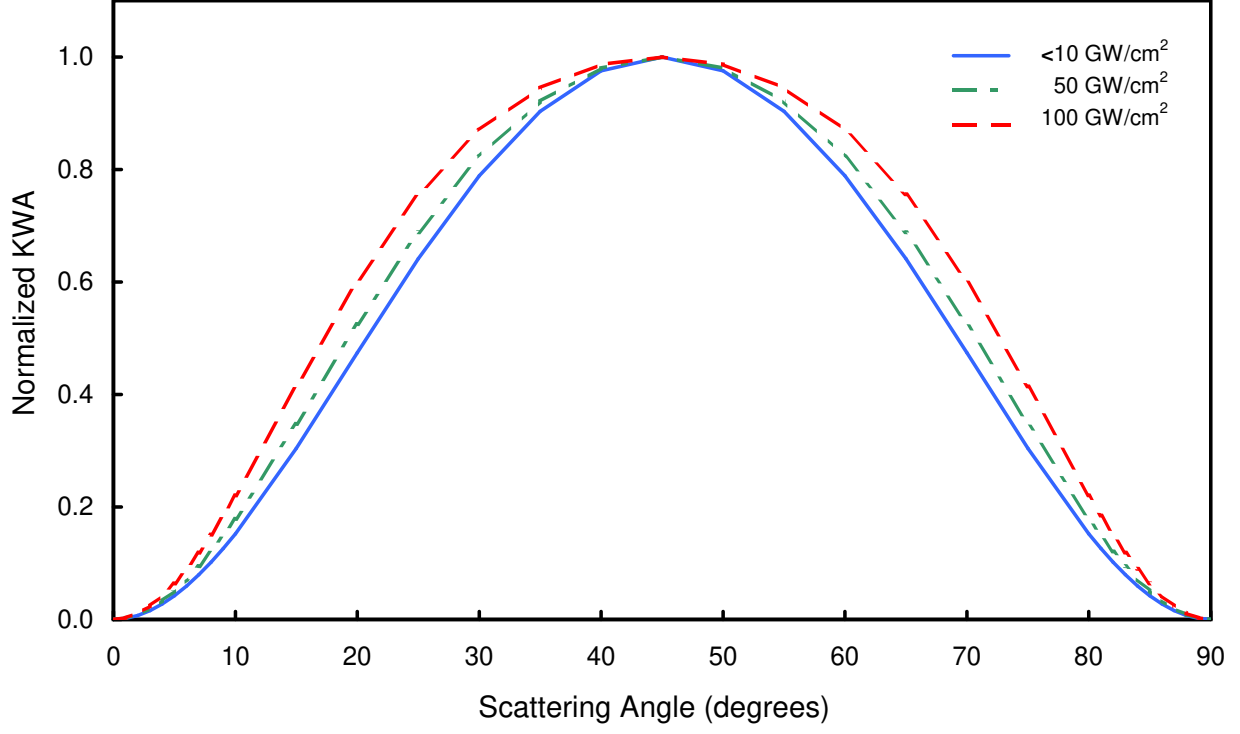
//link.aps.org/doi/10.1103/PhysRev.134.A1210.

FIG. 1: Angular distributions of 350 eV electrons for single photon processes ($\ell = \pm 1$) calculated with the Kroll-Watson approximation (KWA). The results are given as the ratio of the free-free cross section to the field-free cross section, and all calculations are normalized to unity at 45°. The laser polarization direction lies in the scattering plane at 135° to the electron beam (see fig. 2). Calculations for three laser intensities are shown; note that all intensities less than 10 GW/cm^2 result in the solid curve.
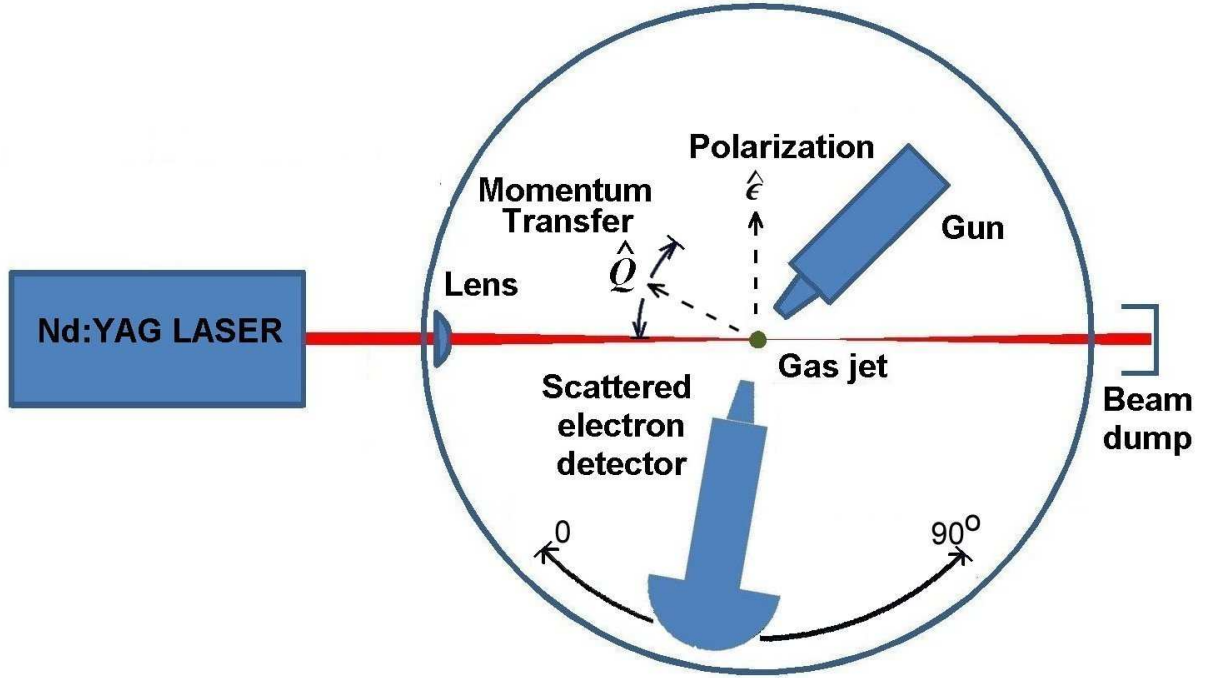
FIG. 2: Schematic of the experimental apparatus showing the relative directions of the laser beam, laser polarization, electron beam, and the momentum transfer. As the scattered electron detector is varied from 0° to 90° the momentum transfer sweeps through 45° as shown; for 90° scattering, it is perpendicular to the polarization direction.
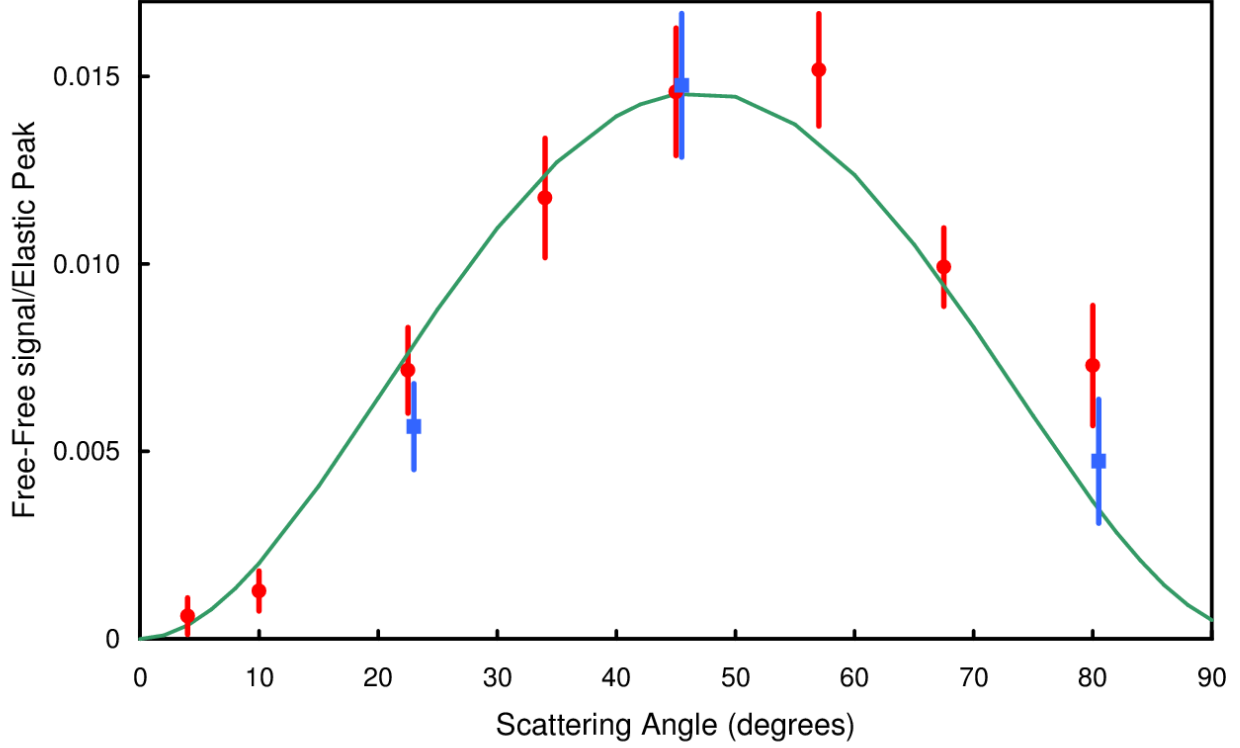
FIG. 3: Free-free angular distribution of 350 eV electrons scattered from an Ar target in the presence of a 1.17 eV laser field. The circles (red) are for a target density of approximately 1 Torr, the squares (blue) are for a target density of approximately 0.1 Torr. The solid (green) line is a Kroll-Watson approximation calculation for single photon processes and polarization 133° to the electron beam. The magnitude of the calculation in the figure corresponds to the best fit to the data. See text for details.